

On the initiation and movement mechanisms of a catastrophic landslide triggered by the 2008 Wenchuan (Ms 8.0) earthquake in the epicenter area

○Shenghua CUI, Gonghui WANG, Xiangjun PEI, Toshitaka KAMAI, Runqiu HUANG

The 2008 Wenchuan earthquake with a surface wave magnitude of 8.0 (Ms8.0) occurred in Sichuan province, SW China (Fig.1). The epicenter area was 80 km west-northwest of Chengdu, the capital city of Sichuan Province. The peak accelerations were 957.7 Gal (EW), 652.9 Gal (SN) and 948.1 Gal (UD) recorded at the epicenter. It was reported that nearly  $2 \times 10^5$  landslides had been triggered by this earthquake (Xu et al. 2003), and 112 landslides with the surface area of each one larger than  $0.5 \text{ km}^2$  were most catastrophic (see Fig.1). Niumiangou landslide triggered in the epicenter area was one of the most catastrophic landslides (Fig.2). The  $7.5 \times 10^6 \text{ m}^3$  mass displaced from a steep slope ( $\sim 30^\circ$ ) adjacent the surface rupture, and traveled  $\sim 2 \text{ km}$  along two gentle ( $< 12^\circ$ ) valleys before coming to rest. Although this landslide had attracted the wide concerns, its initiation and movement mechanisms have been less examined and kept unclear.

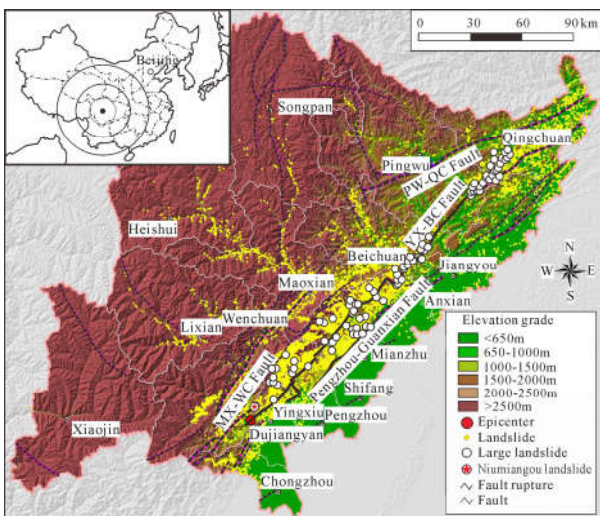


Fig.1 Epicenter of the 2008 Wenchuan earthquake and locations of the coseismic landslides

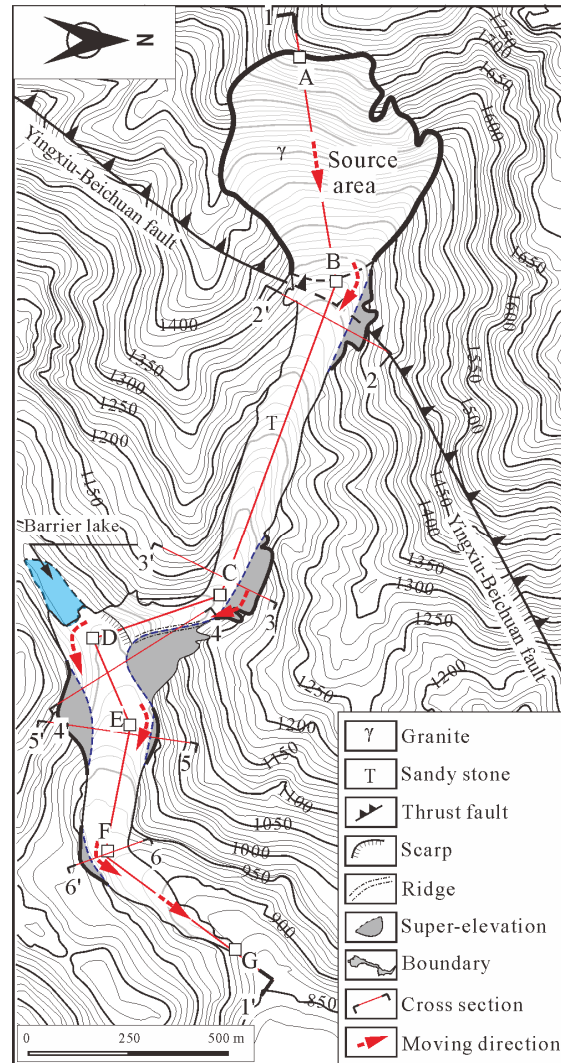


Fig.2 Contour map of Niumiangou landslide area

Site evidences indicated that the landslide was of high mobility with a speed range of 19-36 m/s and an equivalent friction angle of  $\sim 17^\circ$ . From the site observation, we inferred that the initial failure occurred within the water-saturated soil layer on the source area, and liquefaction might have been triggered within the displaced landslide debris, and then enabled the high mobility of the debris from the

source area. Due to the dynamic loading caused by the debris from the source area, the water-saturated colluvial deposit along the travel path might have also been liquefied and then elevated the mobility of displaced debris further. To ensure this inference, we took samples from both the source area and travel path, and performed a series of ring shear tests on them.

Ring-shear tests revealed that the samples from both areas have high potential of liquefaction, and the shear failure can be triggered with high mobility (equivalent friction angle  $<10^\circ$ ) under cyclic loading (material from source area) or impact loading (runout path material) (see Figs.3 and 4). In addition, only a 45 kPa increment of shear stress was required to initiate the shear failure under cyclic loading (see Fig.3), which corresponds to a peak acceleration of about 196 gal. Hence, we concluded that shear failure could be triggered on the landslide materials of the source area due to the introduction of strong seismic motion during the earthquake, and our above-mentioned inferences are reasonable.

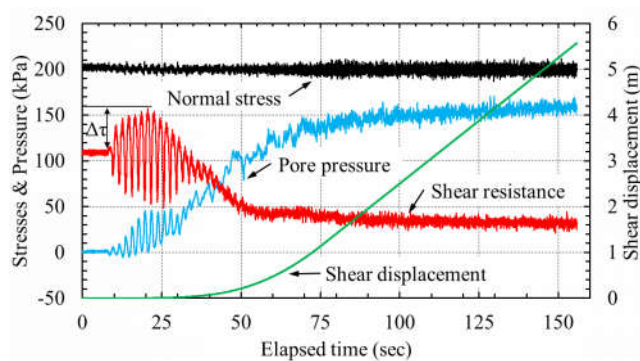


Fig.3 Results of cyclic loading ring-shear test on sample from source area

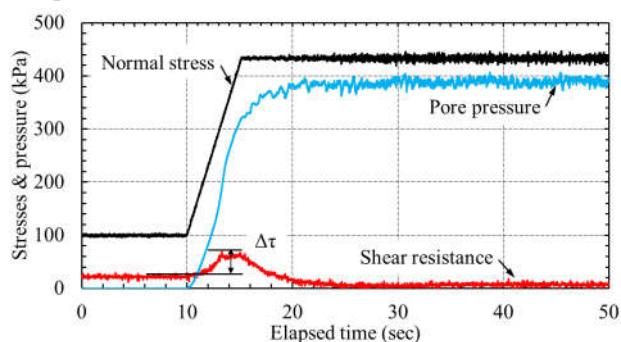


Fig.4 Results of impact loading ring-shear test on sample form runout path

We also used an energy approach to evaluate the occurrence of this landslide. We estimated the total dissipated energy for the shear failure in our cyclic loading test based on an energy approach as used by Sassa et al. (2005). By synthesizing the seismic wave recorded on the main shock of the 2008 Wenchuan earthquake near the epicenter, the seismic energy passing through the potential shear surface of Niuniangou landslide was estimated following the approaches used by Trifunac (2008). We found that the energy, required for the triggering of the shear failure, could be reached around 28 seconds after the beginning of earthquake, and the energy was a very small fraction (~6%) of the total wave energy (see Fig.5). Duration of the wave energy indicated that the landslide most likely occurred during the period of 28-35 seconds. In this period, the wave energy was 60% of the energy throughout the whole duration, and a maximum incident power of ground motion exhibited (see Fig.5).

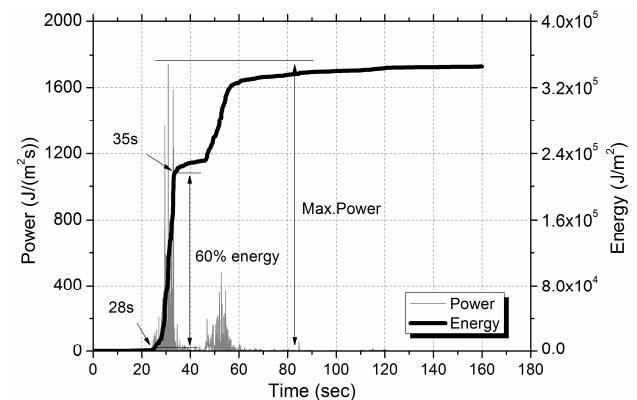


Fig.5 Strong-motion power, wave energy and duration (during 28 to 35 sec), and maximum incident power

Xu, C., Xu, X., Zhou, B., Yu, G., 2013. Nat. Hazards. 69 (3), 1459-1476.

Sassa, K., Wang, G.H., Fukuoka, H., Vankov, D.A., 2005. J. Geotech. Geoenviron. Eng. 131 (6), 750-761.

Trifunac, M.D., 2008. Soil. Dyn. Earthq. Eng. 28 (1), 1-6.